Food Chemistry 237 (2017) 966–973

Contents lists available at ScienceDirect

Food Chemistry

journal homepage: www.elsevier.com/locate/foodchem

Analytical Methods

# Acriflavine-immobilized eggshell membrane as a new solid-state biosensor for Sudan I–IV detection based on fluorescence resonance energy transfer

Ying Li [a], Anyi Wang [a], Yunfei Bai [b], Shiping Wang [a,*]

[a] College of Food Science and Nutritional Engineering, China Agricultural University, 17# Qinghua East Road, Haidian District, Beijing 100083, China
[b] Tianjin Entry-Exit Inspection and Quarantine Bureau, 51# 2nd Street, Tianjin Economic & Technological Development Area (TEDA), Tianjin 300457, China

ARTICLE INFO

*Article history:*
Received 5 November 2016
Received in revised form 15 May 2017
Accepted 7 June 2017
Available online 8 June 2017

*Chemical compounds studied in this article:*
Sudan I (PubChem CID: 5858445)
Sudan II (PubChem CID: 5809936)
Sudan III (PubChem CID: 5379348)
Sudan IV (PubChem CID: 5876571)
Acriflavine (PubChem CID: 14479535)
Glutaraldehyde (PubChem CID: 3485)
Capsanthin (PubChem CID: 5281228)
β-carotene (PubChem CID: 5280489)
Hexane (PubChem CID: 8058)

*Keywords:*
Acriflavine
Eggshell membrane
Solid-surface fluorescence biosensor
Sudan I–IV
Fluorescence resonance energy transfer (FRET)

ABSTRACT

A novel solid-surface fluorescence biosensor for rapid detection of Sudan I–IV was proposed based on fluorescence resonance energy transfer (FRET). The biosensor was fabricated by immobilizing acriflavine (AY) on the eggshell membrane (ESM) with glutaraldehyde as cross-linking agent. FRET mechanism was demonstrated by using AY and Sudan dyes as donor and acceptor respectively, an efficient energy transfer in the present system was indicated by the sufficient spectral overlap integral (J) and proper Förster critical distance ($R_0$). Under optimum conditions, the fluorescence of the AY-ESM could be efficiently quenched by Sudan I–IV and the corresponding linear range was 0.5–60 μM with the detection limits (3σ/slope) of 0.16, 0.26, 0.21 and 0.17 μM respectively. Compared to the detection of Sudan dyes in solution-state, the membrane biosensor exhibited advantages of low detection limits, high sensitivity and selectivity, as well as excellent stability. Recovery tests in spiked real samples also achieved satisfactory results.



## 1. Introduction

Sudan I, II, III and IV (structures are shown in Fig. S1) are a family of lipophilic azo dyes that are widely used in chemical industry for colouring hydrocarbon solvents, oils and waxes (Nohynek, Fautz, Benech-Kieffer, & Toutain, 2004). They are strictly banned for food usage by both the Food Standards Agency and the European Union (Ye, Zhang, Chen, Wang, & Huang, 2014) due to their aftermath of bladder and liver cancer (Stiborova, Martinek, Schmeiser, & Frei, 2006). However, since the bright colour, low cost and stability of Sudan dyes, they are still illegally used as additives in some foodstuffs to improve the appearance, particularly in chilli and ketchup products. Therefore, effective and reliable methods for the rapid detection of Sudan dyes in foodstuffs are of great significance and urgency.

Comparing with the most extensively used methods, such as high performance liquid chromatography (Zhang, Zhang, & Sun, 2006), mass spectrum (Piatkowska, Jedziniak, & Zmudzki, 2016), electroanalytical techniques (Gómez, Arancibia, Aliaga, Núñez, & Rojas-Romo, 2016), terahertz spectroscopy (Qin, Xie, & Ying, 2015) and Raman spectroscopy (Gao et al., 2015), the fluorescent methods have received considerable attention because of their rapid response and high sensitivity. However, recently developed fluorescent probes for Sudan dyes detections are commonly based on metaorganic coordination polymers(Chen et al., 2014; Xue et al., 2016) or synthetic nano-materials (Fang et al., 2016; Li et al.,

* Corresponding author.
*E-mail addresses:* ying_li1992@163.com (Y. Li), 939885301@qq.com (A. Wang), joycekingqhd@sohu.com (Y. Bai), wang744447@sohu.com (S. Wang).

http://dx.doi.org/10.1016/j.foodchem.2017.06.050
0308-8146/

2014). These solution-state materials are sensitive and highly specific in performance but still partly limited by their high cost, complex detection process and susceptibility to solvent effects (Chen et al., 2014; Fang et al., 2016).

In our work, we take the application of solid-surface fluorescent techniques and the eggshell membrane (ESM) is used as the solid matrix. The natural ESM is a subtle network structure with large specific surface area and its fibers are composed mainly of proteins (80–85%) with abundant amino, hydroxyl and carboxyl groups (Tang, Li, Kang, Zhong, & Zhang, 2009), providing favourable conditions for the immobilization and distribution of the probes. Comparing to the above mentioned solution-state probes, ESM matrix of the solid system is cost-effective, portable and stable, based on which large-scale commercialized production and on-site detection could be easily reached.

To form an efficient fluorescent pairs with Sudan I–IV, we immobilized acriflavine (AY) onto ESM as the indicator and the fluorescence mechanism of the detection system was demonstrated as fluorescence resonance energy transfer (FRET). As illustrated in Fig. 1, upon addition of Sudan I–IV, the fluorescence of the acriflavine-immobilized eggshell membrane (AY-ESM) can be efficiently quenched and the fluorescent difference before and after quenching (ΔF) was found proportional to the concentration of Sudan dyes over a wide linear range with low detection limits. In practical application, sample solutions can be directly added on to the membrane after pretreatments and only trace amounts of reagents are required, so the detection process is significantly simplified and the solvent effects could be avoided. To the best of our knowledge, this is the first report on solid-state biosensor for the quantitative detection of Sudan dyes.

## 2. Material and methods

### 2.1. Chemicals and reagents

Sudan I–IV (purity: 99.7%), Capsanthin, β-carotene were purchased from J&K Scientific Ltd. (Beijing, China). Acriflavine (AY) and glutaraldehyde solution (25%, w/w) were purchased from Beijing Chemical Reagent Co. Ltd. (Beijing, China). The fresh eggshells were obtained from De Qingyuan Co. Ltd. (Beijing, China). Unless indicated otherwise, all chemicals were of analytical reagent grade and without further purification. Ultrapure water was prepared in the lab using a Milli Q (Millipore Ltd., USA) water treatment device.

### 2.2. Instrumentation

Fluorescence spectra measurements were performed on an F-7000 fluorescence spectrophotometer (Hitachi Ltd., Japan) with a solid sample holder. The slit (EX/EM) was both 5.0 nm/5.0 nm and the PMT voltage was 700 V. The Ultraviolet–visible (UV–vis) absorption spectra were recorded on Shimadzu UV-1800 UV–vis spectrophotometer (Shimadzu Co. Ltd., China) at the slit of 2 nm using 1 cm quartz cuvettes. Scanning electron microscopic (SEM) images were recorded on a JSM-6360 scanning electron microscopy (JEOL Co. Ltd., Japan) operated at 20 kV with gold sputtered on samples. FTIR spectrum was collected by using Spectrum One FTIR spectrometer in KBr pellet (Perkin-Elmer Wellesley, MA, USA). All of the measurements were operated at room temperature at about 298 K.

### 2.3. Preparation of ESM

ESM was carefully stripped from a broken fresh eggshell and rinsed with copious amount of ultrapure water to completely remove the albumen. Then the membrane was cut into pieces (1 × 1 cm) with a clean cutting nipper and was finally stored in ultrapure water at 277 K for further use.

### 2.4. Immobilization of AY on ESM

About 100 pieces of ESM was immersed in 100 mL, 15% (w/w) glutaraldehyde solution (pH = 8.0) and stirred for 30 min. It was then taken out and rinsed with ultrapure water for five times to remove excess glutaraldehyde. Then the well-washed ESM coated with glutaraldehyde was immersed into 100 mL, 10 μM AY solution (pH = 8.0) and gently stirred for 2 h at 298 K, followed by ultrapure water rinsing for five times. Finally, the glutaraldehyde cross-linked eggshell membrane with immobilized acriflavine (AY-ESM) was dried in a vacuum-constant temperature drying apparatus and stored in a desiccator at 298 K for subsequent use. The experimental procedure for AY immobilization on ESM is summarized in Fig. 2.

### 2.5. Fluorescence measurements

AY-ESM prepared in section 2.4 was moistened with 10 μL ultrapure water and positioned on the surface of a quartz plate.

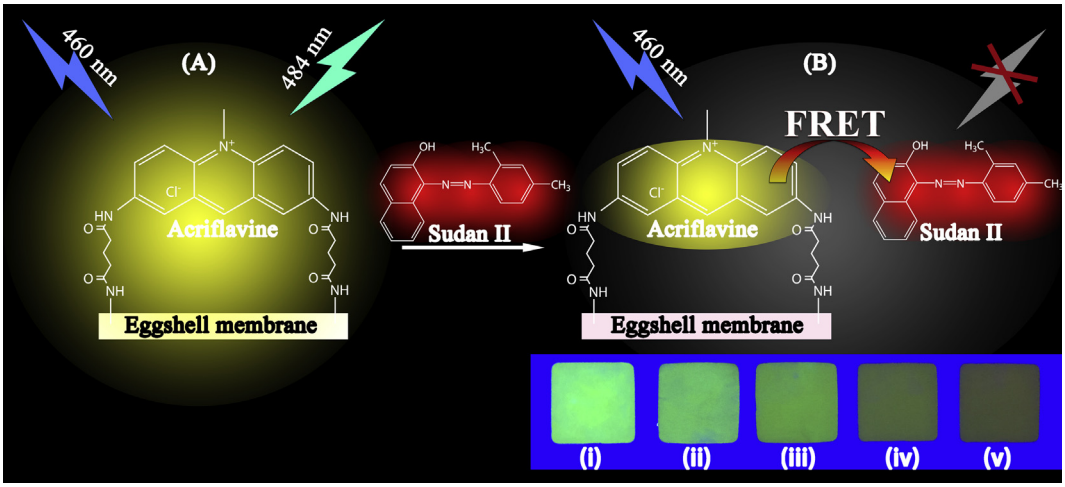


**Fig. 1.** Mechanism for the detection of Sudan I–IV based on FRET. (A) The fluorescence maximum of the AY-ESM appears at 484 nm under continuous excitation at 460 nm. (B) The fluorescence of AY-ESM was quenched by Sudan I–IV through FRET. Inset: Images of AY-ESM for the detection of Sudan II at various concentrations (0, 10, 100, 500, 1000 μM from i to v, 10 μL) under a UV lamp (365 nm).

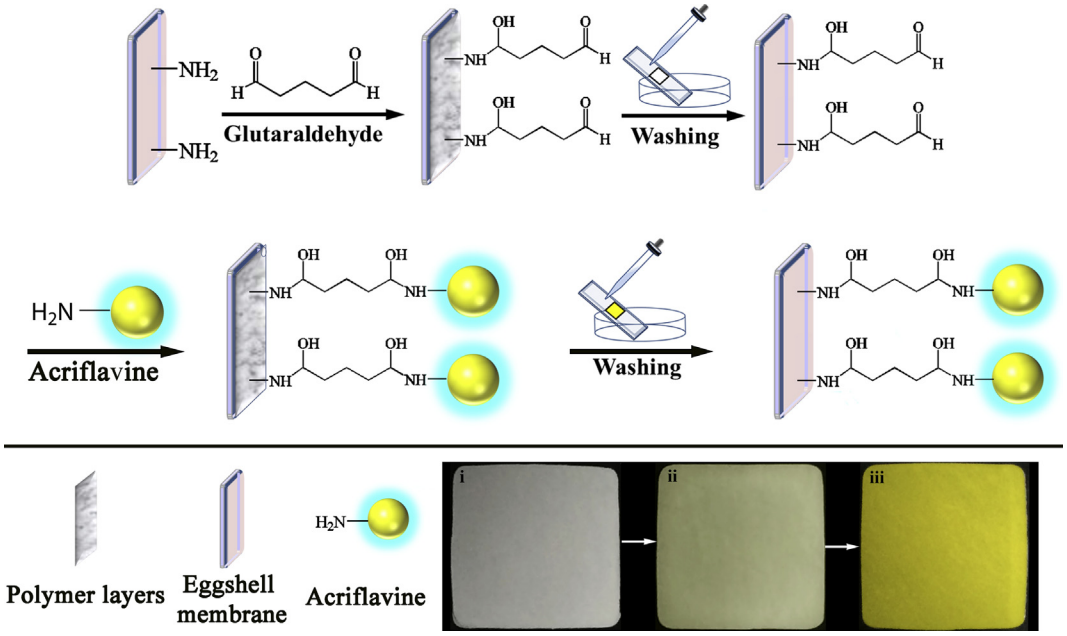


**Fig. 2.** Scheme of AY immobilization on the eggshell membrane. Inset: the photographs of the (i) eggshell membrane, (ii) the glutaraldehyde-crosslinked eggshell membrane and (iii) acriflavine-immobilized eggshell membrane, respectively.

Aliquots of 10 μL different concentrations (0–1000 μM) of Sudan dye were spread evenly on AY-ESM, then the membrane was incubated for 5 min under dark condition. Subsequently, the fluorescence intensity of the membrane was recorded at Ex/Em = 460/484 nm and the fluorescent difference before and after quenching (ΔF) was plotted as the sensor signal.

### 2.6. Pretreatment of real sample

Commercial chilli powder, chilli oil and ketchup samples were purchased from a local supermarket (MerryMart Co. Ltd., Beijing, China) and treated as below. Amount of 1.00 g of the real sample was accurately weighed and added into 20 mL of hexane, then the mixture was vortexed for 5 min and sonicated for 15 min. After being filtrated with a filter membrane (0.45 μm), the obtained filtrate was collected in 50 mL eppendorf tube for the detection of Sudan dyes. For the recovery tests, appropriate amounts of Sudan I–IV were added respectively into the real sample and pretreated through the overall procedure.

### 2.7. Principles of fluorescence resonance energy transfer (FRET)

FRET is a nonradiative process whereby an excited state donor transfers energy to a ground state acceptor (Forster, 1948; Lakowicz, 2006; Sytnik & Litvinyuk, 1996). As revealed by the Förster theory (Lakowicz, 2006), the Förster critical distance ($R_0$) is a constant for each donor–acceptor pair and is defined as the distance that energy transfer (Grant, Xu, Bergeron, & Mroz, 2001), which is given by Eq. (1):

$$R_0^6 = 8.79 \times 10^{-25} k^2 n^{-4} \varnothing_D J \quad (1)$$

where $k$ denotes the average squared orientational part of a dipole-dipole interaction (it is typically assumed that $k^2 = 2/3$ for common organic fluorophores (Lakowicz, 2006)); $n$ is the refractive index of the solvent (n = 1.366); $\Phi_D$ is the fluorescence quantum yield of energy donor in the absence of energy acceptor ($\Phi_D = 0.54$) (Fister, Harris, Rank, & Wacholtz, 1997).

The spectral overlap integral ($J$) expresses the degree of spectral overlap between normalized donor emission and acceptor absorption, which is given by Eq. (2):

$$J = \int_0^\infty F(\lambda)\varepsilon(\lambda)\lambda^4 d\lambda = \frac{\Sigma F(\lambda)\varepsilon(\lambda)\lambda^4 \Delta\lambda}{\Sigma F(\lambda)\Delta\lambda} \quad (2)$$

where F(λ) is the corrected fluorescence emission spectrum of energy donor in the wavelength range from λ to (λ + Δ); ε(λ) is the molar absorption coefficient of energy acceptor at λ; λ is the wavelength.

The spectral overlap integral ($J$) is directly related to the Förster critical distance ($R_0$), which in return affects the energy transfer efficiency ($E$), as shown in Eq. (3):

$$E = R_0^6/(R_0^6 + r^6) \quad (3)$$

where $R_0$ is the Förster critical distance at which the transfer efficiency $E$ = 50%; $r$ is the distance between the energy donor and acceptor.

In principle, the energy transfer efficiency of FRET ($E$) is highly dependent on both the Förster critical distance ($R_0$) and the spectral overlap integral ($J$), where $J$ should be at least greater than 30% and $R_0$ should be in a range of 1–10 nm to make FRET occur (Chen, Mills, & Periasamy, 2003).

## 3. Results and discussion

### 3.1. Characterization of AY-ESM and Sudan I–IV

To understand the influence of cross-linking reaction on the microstructure of the biosensor, ESM and AY-ESM were characterized by scanning electron microscopy (SEM) and Fourier transform infrared spectroscopy (FTIR). As shown in Fig. 3A and B, the immobilization of AY made the fibers rougher with clusters or lumps of cross-linking polymer as compared to the smooth fibers of the natural ESM. However, the mesoporous hierarchical structure of ESM matrix can still be clearly observed after immobilization, indicating that excess reagents were removed completely under continuous stirring and the multiple washing steps. Thus, the interwoven

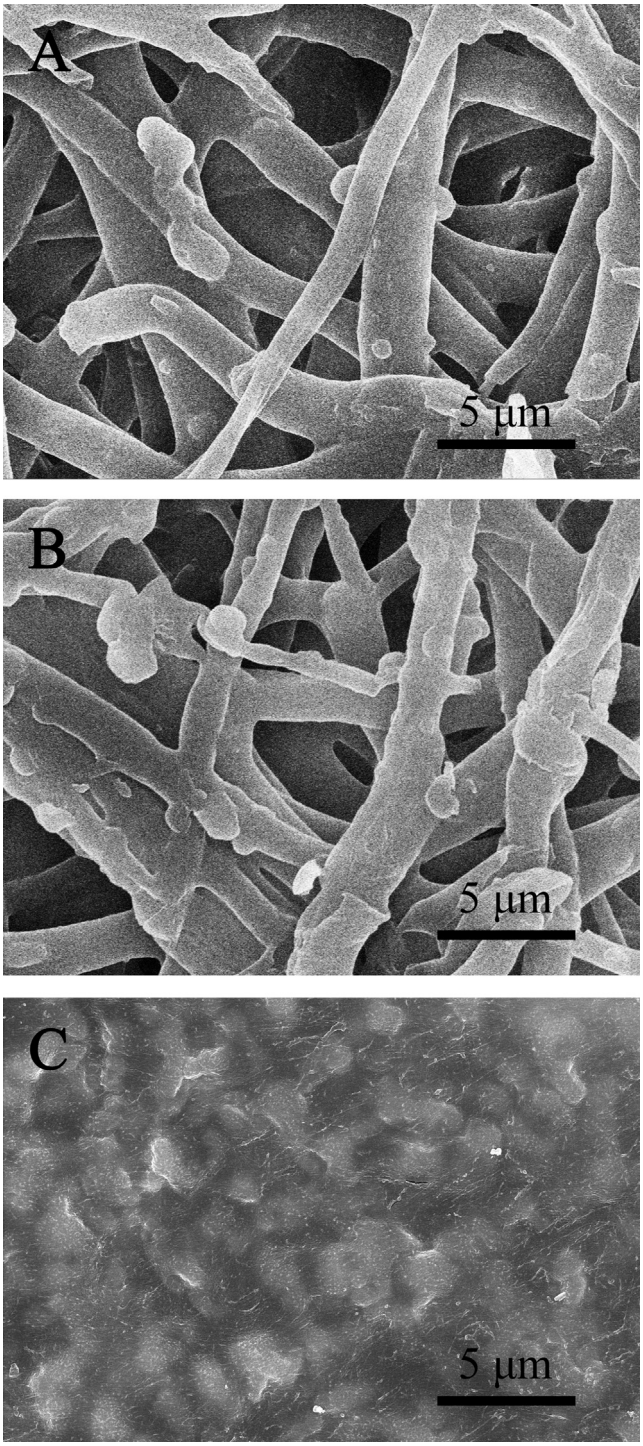


**Fig. 3.** Scanning electron micrographs of (A) eggshell membrane, (B) acriflavine-immobilized eggshell membrane and (C) acriflavine-immobilized eggshell membrane using 25.0% (w/w) glutaraldehyde.

network of ESM with multilayered fibers and pores can provide ideal sites for the combination and distribution of AY as indicator. According to previous studies, it is also possible that the trace amount of Sudan dyes in the working solution can be collected and enriched by the fibrous and porous structure of ESM (Carolina Talio, Alesso, Gimena Acosta, Acosta, & Fernandez, 2014), which would be of great benefit in enhancing the sensitivity of the biosensor. The FTIR analysis of the ESM and AY-ESM are shown in Fig. S2. The major bands for the ESM could be assigned as follows: 3313 $cm^{-1}$ (—OH/—$NH_2$ stretching vibrations); 3071, 2965 and 2877 $cm^{-1}$ (C—H asymmetric stretching vibration in =C—H and =$CH_2$); 1655 $cm^{-1}$ (C=O stretching mode assigned to the amide I vibration); 1528 and 1234 $cm^{-1}$ (C—N stretching/N—H bending modes assigned to amide II vibrations); 1427, 1079 and 633 $cm^{-1}$ (C=C, C—O and C—S stretching vibrations, respectively) (Wang, Li, Wang, & Wang, 2016). Comparing with natural ESM, two new bands at 1200 $cm^{-1}$ (C—O—H deforming vibrations) and 1033 $cm^{-1}$ (C—N stretching of aliphatic I and II amines) appeared in the spectra of AY-ESM after cross-linking, indicating that Schiff base linkages are formed between the aldehyde groups of glutaraldehyde and the amino groups of ESM and AY (Xie & Zang, 2016). In addition, the increase in the relative intensity of the band at 1655 $cm^{-1}$ was corresponded to the C=N stretching vibration of AY, indicating that AY molecules have been successfully immobilized on ESM.

The fluorescence characteristics of AY-ESM in the absence and presence of Sudan I–IV were investigated by two-dimensional and three-dimensional fluorescence spectrum. Herein, Sudan II, with the highest spectral overlap integral ($J$), is used as a representative of Sudan dyes. As shown in Fig. 4B, the fluorescence maximum of AY-ESM appears at 484 nm under continuous excitation at 460 nm. This characteristic peak was associated with AY, which further confirmed the successful immobilization of AY on ESM. Upon addition of Sudan II, the fluorescence intensity decreased efficiently at Ex/Em = 460/484 nm (Fig. 4A), suggesting that AY-ESM could be potentially used as a fluorescence probe to detect Sudan dyes. Fig. S3 shows the time-dependent response of AY-ESM upon addition of Sudan II. The fluorescence intensity at Ex/Em = 460/484 decreased gradually with time and reached equilibrium in about 300 s. Therefore, the fluorescence of AY-ESM in the presence of Sudan dyes were recorded at 5 min.

### 3.2. Mechanism for fluorescence quenching system

To understand the quenching mechanism, UV–vis absorption and fluorescence spectroscopy were utilized to investigate the optical properties of AY-ESM and Sudan dyes. According to the principles of fluorescence spectroscopy, ground-state complex formation will frequently result in perturbation of the absorption spectrum of the fluorophore (Chen et al., 2014). However, by comparing the absorption bands in Fig. 5A (curve b and c), no new absorption peak was found upon addition of Sudan II. Thus the static quenching mechanism based on formation of the ground-state complex is excluded.

As shown in Fig. 5B, the sufficient overlap of the fluorescent emission peak of AY-ESM (curve a) with the UV–vis absorption band of Sudan II (curve b) suggests that fluorescence decrease may arise from the FRET or fluorescence inner filter effect (IFE). According to fluorescence quenching principles, FRET quenching can be influenced by temperature due to the change of molecular collision and the stability of ground state complexes, while IFE is not (Lakowicz, 2006; Ling, Li, Qu, Li, & Luo, 2014). Therefore, $\Delta F$ of AY-ESM towards 40 μM Sudan I–IV (10 μL) was investigated under different temperatures (253 K, 263 K, 273 K, 278 K, 288 K, 298 K, 308 K, 318 K, 323 K) to further determine the possible mechanism. As shown in Fig. S4, even though the temperature exhibit little influence on $\Delta F$ of AY-ESM towards Sudan I–IV, the increasing trend of $\Delta F$ with the increasing of temperature can be seen clearly. Therefore, the fluorescence quenching of AY-ESM by Sudan dyes should be mainly caused by FRET, rather than IFE, with AY molecules as the energy donor and Sudan I–IV as the energy acceptor.

To further investigate the FRET mechanism, FRET parameters were calculated according to Eqs. (1)–(3) provided in section 2.7. The spectral overlap integral ($J$) was calculated to be

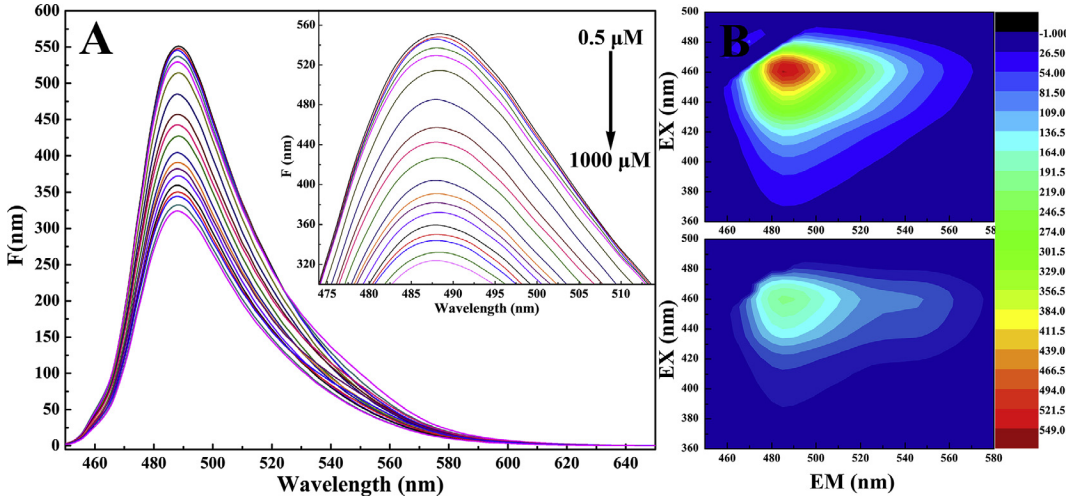


**Fig. 4.** (A) Fluorescence emission spectra of the AY-ESM in the presence of different concentrations of Sudan II (0, 0.5, 1, 5, 10, 20, 40, 60, 80, 100, 150, 200, 250, 300, 400, 500, 600, 800 and 1000 μM from 1 to 19, 10 μL) under optimum conditions. (B) three-dimensional fluorescence spectrum of AY-ESM in the absence and presence of 1000 μM Sudan II (10 μL). T = 298 K.

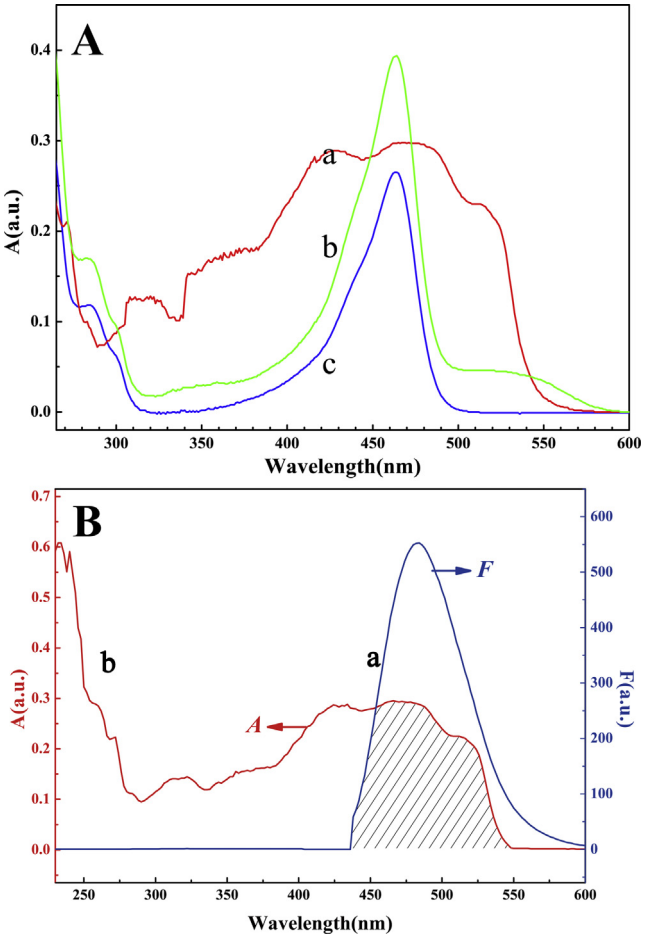


**Fig. 5.** (A) UV–vis absorption spectra of the 10 μM AY (a), 40 μM Sudan II (b), and the mixture of 10 μM AY and 40 μM Sudan II (c). (B) The fluorescence emission spectra of the AY-ESM (glutaraldehyde, 15%, w/w; AY, 10 μM; pH = 8.0) under continuous excitation at 460 nm (a) and the UV–vis absorption spectra of 40 μM Sudan II (b). T = 298 K.

$6.29 \times 10^{-16}$ cm$^3$ L mol$^{-1}$ by Eq. (2). The Förster critical distance ($R_0$) and the distance between the donor and acceptor ($r$) were both calculated to be 2 nm by Eqs. (2) and (3), which is short enough to allow efficient FRET from AY-ESM to Sudan dyes. According to references, acridine and azobenzene derivatives have been widely employed as energy donors or acceptors to build FRET sensors (Chen et al., 2014; Farzampour & Amjadi, 2014; Kong et al., 2017), which can be ascribed to their intrinsic structural advantageous. Acridine derivatives are a class of macrocyclic compounds with rigid conjugate structure, thus a long-range dipole-dipole interaction may take place between the acridine moiety of AY as a donor molecule and some appropriate guests as acceptor molecules via through-space energy transfer (Zhang, Han, Chen, Zhang, & Liu, 2013). Some studies have also shown that a synergistic interplay between the π-conjugation and the intramolecular hydrogen bond of azobenzene derivatives, such as Sudan dyes, might contribute to the remarkable activity of such compounds and facilitates the mechanistically required energy transfer step (Jo et al., 2012). In addition, the distance ($R_0$) and overlap integral ($J$) requirements of FRET system can be easily satisfied through a series of reduction reactions, during which the azo bond could be cleaved to generate a suitable donor-acceptor distance and UV–vis absorption band (Kiyose et al., 2010). In summary, all the evidence indicated that the fluorescence quenching of AY-ESM by Sudan dyes in this study is predominantly attributed to FRET.

### 3.3. Optimization of conditions for the detection of Sudan I–IV

#### 3.3.1. Effect of concentration of glutaraldehyde

Glutaraldehyde has been used for several decades as an effective cross-linking agent of ESM (Li et al., 2017; Wang, Bai, Gao, & Wang, 2015; Zheng et al., 2011), the mechanism of which is mainly contributed to the effect of aldehyde-amine condensation between the functional groups of ESM protein and the target compounds. According to the SEM image of AY-ESM cross-linked by 25% (w/w) glutaraldehyde (Fig. 3C) and our previous study (Wang et al., 2015), a thick layer of cross-linking polymer would form on the surface of ESM when the glutaraldehyde concentration reaches 25% (w/w). Thus in order to protect the natural microstructure of ESM, the effect of glutaraldehyde concentration on the fluorescence intensity of AY-ESM was studied over the range of 1%–25% (w/w).

It can be seen from Fig. S5-A that the fluorescence intensity of AY-ESM increased with the increasing concentration of glutaraldehyde at first and remain unchanged after the concentration of glutaraldehyde exceeded 15% (w/w), indicating that the amount of the

cross-linking agent is not enough to bind all AY molecules onto the membrane at the beginning and gradually reached saturation afterwards. Therefore, 15% (w/w) glutaraldehyde was chosen for AY immobilization on ESM.

### 3.3.2. Effect of concentration of AY

According to references (Guo, Zhang, Zhao, Wang, & Xu, 1997; Weill & Calvin, 1963), the self-quenching effect would occur when the fluorescent dyes like AY are at a high concentration about $10^{-6}$ M, during which the dye monomers aggregate and form dimers (AY-AY) with a certain angle (Guo et al., 1997). In this study, the forming of such dimers is extremely unfavorable for the detection of Sudan dyes. On one hand, the plane property of molecule is destroyed by the angle, leading to the decrease in the fluorescence of AY. On another, the space hinder of AY-AY makes it hard for Sudan dyes to get close, resulting in the decrease of sensitivity (Liu, Sa, Hu, & Kong, 2006). Therefore, in order to avoid the self-quenching effect, the concentration of AY in the immobilization step was optimized over the range of 0.1 to 25 μM. As expected, increasing the concentration of AY from 0.1 to 10 μM increased the obtained fluorescence signal of AY-ESM (Fig. S5-B), but when the concentration of AY exceeded 10 μM, the fluorescence intensity decreased sharply due to the self-quenching effect. Hence, the optimum concentration of AY was chosen as 10 μM.

By comparing this result to previous studies of AY in solution-state (Pérez-Ruiz, Martínez-Lozano, Sanz, & San Miguel, 1997), we found that the self-quenching concentration of AY has been greatly increased when immobilized on ESM. Since the dispersion and enrichment effects provided by the entangled structure of ESM fibers has been reported in many fields of application such as the synthesis of nanoparticles (Liang et al., 2014; Zheng et al., 2011) and the adsorption of water contaminants(Abdel-Khalek, Rahman, & Francis, 2017; Wang et al., 2017). It is reasonable to expect that the ESM fibers might have the ability to disperse AY molecules and thus avoid the molecules from coming too close. The effective enhancement of AY concentration as the indicator on solid matrix can improve the sensitivity of the biosensor, which could be considered as another advantage of the proposed method.

### 3.3.3. Effect of pH value

Since the cross-linking effect of glutaraldehyde is highly pH dependent, the pH of the cross-linking solutions (including glutaraldehyde solution and AY solution) was optimized over the pH range of 2.0–12.0. It is seen from Fig. S5-C that the fluorescence intensity of AY-ESM increased with increasing pH at first, and then decreased when the pH is beyond 8.0. This phenomenon can be explained by the cross-linking process of glutaraldehyde and ESM. When monomeric glutaraldehyde interact with the amino groups of ESM protein, a nucleophilic attack occurs on the aldehyde groups to yield a non-conjugated Schiff base (Goldstein & Manecke, 1976; Wang et al., 1998), which is considered to be unstable under acidic conditions. Therefore, the optimum pH values of glutaraldehyde solution and AY solution were determined to be 8.0.

### 3.4. Sensitivity and selectivity for Sudan I–IV detection

According to the optimum conditions above, the sensitivity of AY-ESM toward Sudan I–IV was investigated. As illustrated in Figs. 6 and S6, the fluorescent difference before and after quenching (ΔF) at Ex/Em = 460/484 nm against the concentrations of Sudan I–IV shows good linear relationships over the range of 0.5–60 μM, with the satisfactory correlation coefficients ($R^2$) of 0.9895 for Sudan I, 0.9967 for Sudan II, 0.9938 for Sudan III and 0.9959 for Sudan IV. Low detection limits (3σ/slope) were also

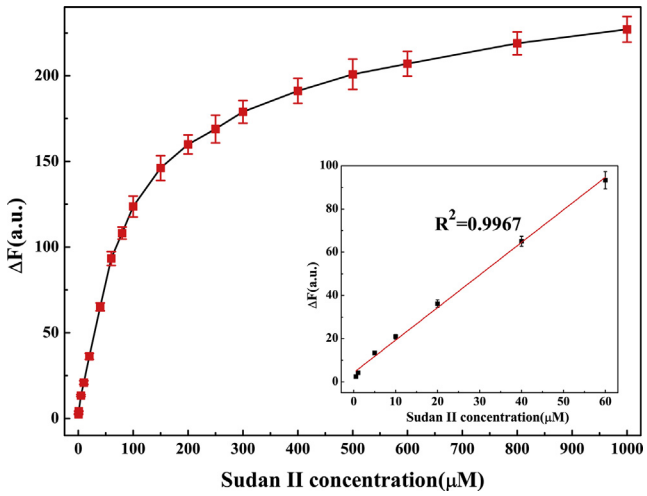


**Fig. 6.** Relationship between the fluorescent difference in the presence and absence of Sudan II (ΔF) and the concentration of Sudan II. Inset: the linear region of 0.5–60 μM Sudan II. Excitation wavelength: 460 nm. The error bars denote the standard deviation of the values obtained with the three same assays. T = 298 K.

obtained at 0.16, 0.26, 0.21, and 0.17 μM for Sudan I–IV, respectively.

To further demonstrate the selectivity of AY-ESM biosensor, the fluorescence response of potentially interfering substances that are expected to coexist in chilli and ketchup products (such as Vitamin C, Capsanthin, β-carotene, sodium citrate, saccharides and metal ions) or ESM (such as amino acid and $Ca^{2+}$) were tested. As shown in Fig. S7, the addition of 40 μM Sudan I–IV (10 μL) onto AY-ESM biosensor caused an obvious change in the value of ΔF, but most of the interfering substances like pigments, amino acids and sugars could not lead to any significant fluorescence change (<5%) even at a rather high concentration. Additionally, ΔF towards Sudan I–IV in the presence of those substances also produced slight interference (<8%), indicating that the presence of those substances does not inhibit FRET of the detection system and thus demonstrate good selectivity toward Sudan dyes. However, the fluorescence quenching was mostly caused by some divalent cations, especially $Cu^{2+}$ and $Ca^{2+}$. Thus, a proper separation or pretreatment would be necessary when the proposed method was put into practice.

### 3.5. Prediction of spiked samples

To verify the applicability of the proposed method, AY-ESM was employed to detect Sudan I–IV in real chilli powder, chilli oil and ketchup samples, which were pretreated and analyzed in accordance with procedures described in section 2.6 and 2.5. It was satisfactory that Sudan II in one ketchup sample (Fig. S8) were actually found and determined with the concentration of 3.2 μM by this method. Reasonable spike recoveries were also obtained by adding standard solutions of Sudan I–IV with three different concentrations (10, 20, 60 μM). As shown in Table S1, the recoveries of chilli powder, chilli oil and ketchup samples were in the ranges of 96.4–104.7%, 94.9–102.8% and 95.4–105.1% with RSDs (n = 5) of 1.0–5.9% for chilli powder, 1.1–5.6% for chilli oil and 1.1–6.2% for ketchup respectively, indicating that the proposed method is potentially applicable and reliable for the detection of Sudan I–IV in real samples.

In order to evaluate the performances, the proposed method was compared with some literature methods for the analysis of Sudan dyes and the results are presented in Table S2. Compared with the previously reported methods, the proposed method exhibits low detection limits, good linearity, satisfactory recovery and

superiorities in the consumption of samples, organic solvents and equipments. From all the results obtained above, it is clear that the proposed method is a simple, accurate and reliable technique, and is suitable for the analysis of various Sudan dyes in the food and adulteration samples.

### 3.6. Stability of AY-ESM

Considering to the actual practice, the stability of AY-ESM is of particular importance as they may often be stored for weeks or months prior to use. Since ESM protein is easy to be contaminated by microorganism in moist environment, the prepared AY-ESM was fully dried and stored in a desiccator (as described in section 2.4) to avoid activity decrease. In order to determine the long-term stability of the biosensor, the fluorescence intensity change of AY-ESM was monitored periodically for 60 days. As shown in Fig. S9, the fluorescence signals of AY-ESM decreased gradually to 80% of its initial values after being stored 15 days and then basically remained at 78.7% in the next 45 days. This result was compared with other methods reported in the literature, newly developed sensing materials immobilized by glutaraldehyde, polymers, enzymes and nanoparticles were selected as references. As shown in Table S3, the remained activity of the present method is higher than or at least similar to that of the other methods, especially with regard to the long-term storage after 15 days. In addition, the storage condition of the present method is much easier to be achieved compared with the specific temperature, humidity, pH and buffer requirements of literature methods, which could be considered as a significant advantage in commercial production and possible industrial applications.

## 4. Conclusions

In summary, we have successfully immobilized AY onto ESM to develop a novel solid-surface fluorescence biosensor for the rapid detection of Sudan I–IV. Under optimum conditions, AY-ESM biosensor towards Sudan I–IV exhibit good linearity and low detection limits. Recovery tests in spiked real samples and interference study towards some potentially interfering substances also achieved satisfactory results. This is the first demonstration and utilization of solid-state biosensor accompanied with the FRET method for the quantitative detection of Sudan dyes. With ESM as the solid matrix, the proposed method shows many promising features, such as cost-efficiency, good stability, easy operation and free of solvent effects, etc. Further investigation may lead to an extension of this system for the detection of other dyes or food additives.

## Conflict of interest statement

We wish to confirm that there are no known conflicts of interest associated with this manuscript and there has been no significant financial support for this work that could have influenced its outcome.

We confirm that the manuscript has been read and approved by all named authors and that there are no other persons who satisfied the criteria for authorship but are not listed. We further confirm that the order of authors listed in the manuscript has been approved by all of us.

## Acknowledgements

This work was supported by the Project of Construction of Food Supervision System and Research on Food Quality HACCP in Chaoyang District [No. 25012152]. The authors thank Jiaxi Fang and Yun Zhou for providing language help. We also acknowledge the experimental contributions of Xuejun Li and Juan Song.

## Appendix A. Supplementary data

Supplementary data associated with this article can be found, in the online version, at http://dx.doi.org/10.1016/j.foodchem.2017.06.050.

## References

Abdel-Khalek, M. A., Rahman, M. K. A., & Francis, A. A. (2017). Exploring the adsorption behavior of cationic and anionic dyes on industrial waste shells of egg. *Journal of Environmental Chemical Engineering, 5*(1), 319–327.

Carolina Talio, M., Alesso, M., Gimena Acosta, M., Acosta, M., & Fernandez, L. P. (2014). Sequential determination of lead and cobalt in tap water and foods samples by fluorescence. *Talanta, 127*, 244–249.

Chen, N. Y., Li, H. F., Gao, Z. F., Qu, F., Li, N. B., & Luo, H. Q. (2014). Utilizing polyethyleneimine-capped silver nanoclusters as a new fluorescence probe for Sudan I-IV sensing in ethanol based on fluorescence resonance energy transfer. *Sensors and Actuators B: Chemical, 193*, 730–736.

Chen, Y., Mills, J. D., & Periasamy, A. (2003). Protein localization in living cells and tissues using FRET and FLIM. *Differentiation, 71*(9–10), 528–541.

Fang, A., Long, Q., Wu, Q., Li, H., Zhang, Y., & Yao, S. (2016). Upconversion nanosensor for sensitive fluorescence detection of Sudan I–IV based on inner filter effect. *Talanta, 148*, 129–134.

Farzampour, L., & Amjadi, M. (2014). Sensitive turn-on fluorescence assay of methimazole based on the fluorescence resonance energy transfer between acridine orange and silver nanoparticles. *Journal of Luminescence, 155*, 226–230.

Fister, J. C., Harris, J. M., Rank, D., & Wacholtz, W. (1997). Molecular photophysics of acridine yellow studied by phosphorescence and delayed fluorescence – An undergraduate physical chemistry experiment. *Journal of Chemical Education, 74*(10), 1208–1212.

Forster, T. (1948). Zwischenmolekulare Energiewanderung und Fluoreszenz (Intermolecular energy transfer and fluorescence). *Annalen Der Physik, 2*(1–2), 55–75.

Gao, F., Hu, Y., Chen, D., Li-Chan, E. C. Y., Grant, E., & Lu, X. (2015). Determination of Sudan I in paprika powder by molecularly imprinted polymers–thin layer chromatography–surface enhanced Raman spectroscopic biosensor. *Talanta, 143*, 344–352.

Goldstein, L., & Manecke, G. (1976). *The chemistry of enzyme immobilization*. New York: Academic press.

Gómez, M., Arancibia, V., Aliaga, M., Núñez, C., & Rojas-Romo, C. (2016). Determination of Sudan I in drinks containing Sunset yellow by adsorptive stripping voltammetry. *Food Chemistry, 212*, 807–813.

Grant, S. A., Xu, J. T., Bergeron, E. J., & Mroz, J. (2001). Development of dual receptor biosensors: An analysis of FRET pairs. *Biosensors & Bioelectronics, 16*(4–5), 231–237.

Guo, X. Q., Zhang, Z. L., Zhao, Y. B., Wang, D. Y., & Xu, J. G. (1997). DNA-dye fluorescence enhancement based on shifting the dimer-monomer equilibrium of fluorescent dye. *Applied Spectroscopy, 51*(7), 1002–1007.

Jo, J., Lee, H. Y., Liu, W., Olasz, A., Chen, C.-H., & Lee, D. (2012). Reactivity-based detection of Copper(II) ion in water: Oxidative cyclization of azoaromatics as fluorescence turn-on signaling mechanism. *Journal of the American Chemical Society, 134*(38), 16000–16007.

Kiyose, K., Hanaoka, K., Oushiki, D., Nakamura, T., Kajimura, M., Suematsu, M., et al. (2010). Hypoxia-sensitive fluorescent probes for in vivo real-time fluorescence imaging of acute ischemia. *Journal of the American Chemical Society, 132*(45), 15846–15848.

Kong, L., Zhu, J., Wang, W., Jin, L., Fu, Y., Duan, B., et al. (2017). Highly sensitive turn-on fluorescence detection of thrombomodulin based on fluorescence resonance energy transfer. *Spectrochimica Acta Part A: Molecular and Biomolecular Spectroscopy, 173*, 675–680.

Lakowicz, J. R. (2006). *Principles of fluorescence spectroscopy*. New York: Springer, US.

Li, Q., Bai, Y., Jin, T., Wang, S., Cui, W., & Stanciulescu, I. (2017). Bioinspired engineering of poly(ethylene glycol) hydrogels and natural protein fibers for layered heart valve constructs. *ACS Applied Materials & Interfaces*. http://dx.doi.org/10.1021/acsami.7b03281.

Li, N., Gu, Y., Gao, M., Wang, Z., Xiao, D., & Li, Y. (2014). Label-free silver nanoparticles for visual colorimetric detection of etimicin. *Analytical Methods, 6*(19), 7906–7911.

Liang, M., Su, R., Qi, W., Yu, Y., Wang, L., & He, Z. (2014). Synthesis of well-dispersed Ag nanoparticles on eggshell membrane for catalytic reduction of 4-nitrophenol. *Journal of Materials Science, 49*(4), 1639–1647.

Ling, Y., Li, J. X., Qu, F., Li, N. B., & Luo, H. Q. (2014). Rapid fluorescence assay for Sudan dyes using polyethyleneimine-coated copper nanoclusters. *Microchimica Acta, 181*(9–10), 1069–1075.

Liu, S. P., Sa, C., Hu, X. L., & Kong, L. (2006). Fluorescence quenching method for the determination of sodium carboxymethyl cellulose with acridine yellow or acridine orange. *Spectrochimica Acta Part A Molecular and Biomolecular Spectroscopy, 64*(4), 817–822.

Nohynek, G. J., Fautz, R., Benech-Kieffer, F., & Toutain, H. (2004). Toxicity and human health risk of hair dyes. *Food and Chemical Toxicology, 42*(4), 517–543.

Pérez-Ruiz, T., Marínez-Lozano, C., Sanz, A., & San Miguel, M. T. (1997). Flow extraction spectrophotometric method for the determination of diclofenac sodium in pharmaceutical preparations. *Journal of Pharmaceutical and Biomedical Analysis, 16*(2), 249–254.

Piatkowska, M., Jedziniak, P., & Zmudzki, J. (2016). Multiresidue method for the simultaneous determination of veterinary medicinal products, feed additives and illegal dyes in eggs using liquid chromatography-tandem mass spectrometry. *Food Chemistry, 197*(Part A), 571–580.

Qin, J., Xie, L., & Ying, Y. (2015). Determination of tetracycline hydrochloride by terahertz spectroscopy with PLSR model. *Food Chemistry, 170*, 415–422.

Stiborova, M., Martinek, V., Schmeiser, H. H., & Frei, E. (2006). Modulation of CYPlA1-mediated oxidation of carcinogenic azo dye Sudan I and its binding to DNA by cytochrome b(5). *Neuroendocrinology Letters, 27*, 35–39.

Sytnik, A., & Litvinyuk, I. (1996). Energy transfer to a proton-transfer fluorescence probe: Tryptophan to a flavonol in human serum albumin. *Proceedings of the National Academy of Sciences of the United States of America, 93*(23), 12959–12963.

Tang, J., Li, J., Kang, J., Zhong, L., & Zhang, Y. (2009). Preliminary studies of application of eggshell membrane as immobilization platform in sandwich immunoassay. *Sensors and Actuators B: Chemical, 140*(1), 200–205.

Wang, A., Bai, Y., Gao, H., & Wang, S. (2015). A tetracycline-selective fluorescent biosensor using anthranilic acid immobilized on a glutaraldehyde-coated eggshell membrane. *Analytical Methods, 7*(16), 6842–6847.

Wang, A., Li, Y., Wang, T., & Wang, S. (2016). Copper ion-selective fluorescent sensor using salicyl fluorone immobilized on a glutaraldehyde-coated eggshell membrane. *Analytical Methods, 8*(9), 2112–2117.

Wang, Q., Ma, C., Li, W., Fan, M., Li, S., & Ma, L. (2017). $MnO_2$ submicroparticles from chinese brush and their application in treatment of methylene blue contaminated wastewater. *Acta Chimica Slovenica, 64*(1), 55–62.

Wang, Z. M., Zhu, G. Y., Huang, Q. C., Qian, M. X., Shao, M. C., Jia, Y. S., & Tang, Y. Q. (1998). X-ray studies on cross-linked lysozyme crystals in acetonitrile-water mixture. *Biochimica Et Biophysica Acta-Protein Structure and Molecular Enzymology, 1384*(2), 335–344.

Weill, G., & Calvin, M. (1963). Optical properties of chromophore-macromolecule complexes – Absorption and fluorescence of acridine dyes bound to polyphosphates and dna. *Biopolymers, 1*(5), 401–417.

Xie, W., & Zang, X. (2016). Immobilized lipase on core-shell structured Fe3O4-MCM-41 nanocomposites as a magnetically recyclable biocatalyst for interesterification of soybean oil and lard. *Food Chemistry, 194*, 1283–1292.

Xue, S.-F., Lu, L.-F., Wang, Q.-X., Zhang, S., Zhang, M., & Shi, G. (2016). An integrated logic system for time-resolved fluorescent "turn-on" detection of cysteine and histidine base on terbium (III) coordination polymer–copper (II) ensemble. *Talanta, 158*, 208–213.

Ye, X., Zhang, J., Chen, H., Wang, X., & Huang, F. (2014). Fluorescent nanomicelles for selective detection of Sudan dye in pluronic F127 aqueous media. *ACS Applied Materials & Interfaces, 6*(7), 5113–5121.

Zhang, Y.-M., Han, M., Chen, H.-Z., Zhang, Y., & Liu, Y. (2013). Reversible molecular switch of acridine red by triarylpyridine-modified cyclodextrin. *Organic Letters, 15*(1), 124–127.

Zhang, Y., Zhang, Z., & Sun, Y. (2006). Development and optimization of an analytical method for the determination of Sudan dyes in hot chilli pepper by high-performance liquid chromatography with on-line electrogenerated BrO-luminol chemiluminescence detection. *Journal of Chromatography A, 1129*(1), 34–40.

Zheng, B., Xie, S., Qian, L., Yuan, H., Xiao, D., & Choi, M. M. F. (2011). Gold nanoparticles-coated eggshell membrane with immobilized glucose oxidase for fabrication of glucose biosensor. *Sensors and Actuators B: Chemical, 152*(1), 49–55.